Neuro-Oncology 14(4):426–439, 2012.
doi:10.1093/neuonc/nos055
Advance Access publication March 6, 2012

NEURO-ONCOLOGY

Expression of podoplanin in human astrocytic brain tumors is controlled by the PI3K-AKT-AP-1 signaling pathway and promoter methylation

Heike Peterziel, Julia Müller, Andreas Danner, Sebastian Barbus, Hai-Kun Liu, Bernhard Radlwimmer, Torsten Pietsch, Peter Lichter, Günther Schütz, Jochen Hess, and Peter Angel

Divisions of Signal Transduction and Growth Control, DKFZ/ZMBH Alliance (H.P., J.M., J.H., P.A.), Molecular Genetics, DKFZ (A.D., S.B., B.R., P.L.), Molecular Biology of the Cell I, DKFZ/ZMBH Alliance (H.-K.L., G.S.), Heidelberg, Germany; Department of Neuropathology, University of Bonn, Bonn, Germany (T.P.); Junior Research Group Molecular Mechanisms of Head and Neck Tumors, DKFZ/ZMBH Alliance, Heidelberg, Germany (J.H.); Research Group Experimental Head and Neck Oncology, Department of Otolaryngology, Head and Neck Surgery, University Hospital Heidelberg, Heidelberg, Germany (J.H.)

Recently, we found strong overexpression of the mucin-type glycoprotein podoplanin (PDPN) in human astrocytic brain tumors, specifically in primary glioblastoma multiforme (GB). In the current study, we show an inverse correlation between PDPN expression and PTEN levels in primary human GB and glioma cell lines, and we report elevated PDPN protein levels in the subventricular zone of brain tissue sections of PTEN-deficient mice. In human glioma cells lacking functional PTEN, reintroduction of wild-type PTEN, inhibition of the PTEN downstream target protein kinase B/AKT, or interference with transcription factor AP-1 function resulted in efficient downregulation of PDPN expression. In addition, we observed hypoxia-dependent PDPN transcriptional control and demonstrated that PDPN expression is subject to negative transcriptional regulation by promoter methylation in human GB and in glioma cell lines. Treatment of PTEN-negative glioma cells with demethylating agents induced expression of PDPN. Together, our findings show that increased PDPN expression in human GB is caused by loss of PTEN function and activation of the PI3K-AKT-AP-1 signaling pathway, accompanied by epigenetic regulation of *PDPN* promoter activity. Silencing of PDPN expression leads to reduced proliferation and migration of glioma cells, suggesting a functional role of PDPN in glioma progression and malignancy. Thus, specific targeting of PDPN expression and/or function could be a promising strategy for the treatment of patients with primary GB.

Keywords: glioma, Jun, podoplanin, promoter methylation, PTEN.

Glioblastoma multiforme (GB) World Health Organization (WHO) grade IV is the most common primary brain tumor in humans. This tumor is characterized by a highly anaplastic, astrocytic phenotype and is associated with very poor prognosis. Until recently, GB have been subdivided mainly into primary tumors, characterized by de novo manifestation, and secondary tumors with a history of prior lower-grade infiltrating astrocytoma.[1] These tumor entities evolve through different genetic pathways. Frequent alterations in primary GB include epidermal growth factor receptor (*EGFR*) gene amplification, loss of the tumor-suppressor genes *CDKN2A/p16*^{INK4a} and *p14*^{ARF}, and inactivation of mutations in or genetic loss of *PTEN* (phosphatase and tensin homologue deleted on chromosome 10), whereas secondary GB more often presents with activation of mutations in the platelet-derived growth factor receptor gene (*PDGFR*) and inactivation of the *TP53* and

Received January 31, 2011; accepted December 23, 2011.

Corresponding Author: Dr. Heike Peterziel, Division of Signal Transduction and Growth Control, German Cancer Research Center Heidelberg, Im Neuenheimer Feld 280, D-69120 Heidelberg, Germany (h.peterziel@dkfz.de).

retinoblastoma (*RB1*) tumor-suppressor genes. Furthermore, mutation of isocitrate dehydrogenase (IDH) often occurs in secondary GB but only infrequently in primary GB[2] (for recent reviews see[1,3]). Genetic profiling data on large collections of human tumors have provided evidence for the presence of different signatures of primary GB based on genetic and epigenetic patterns of gene regulation. At present, there seem to be 2 major tumor subgroups,[4,5] which possibly can be further subdivided[6,7] (for review see[8]). Further complexity is added by the fact that epigenetic methylation also may distinguish between glioma subgroups and may be correlated with the clinical outcome of cancer therapy and survival among patients with GB. Recently, this has led to the postulation of the existence of another glioma subgroup with a glioma-CpG island methylator phenotype (G-CIMP).[9]

One gene that is significantly associated with the mesenchymal GB signature encodes the mucin-like transmembrane glycoprotein podoplanin (*PDPN*). Podoplanin has been named according to its function in shaping podocytes in kidney glomeruli;[10] however, the protein has been additionally described in a variety of biological contexts under different names (eg, T1a in alveolar epithelial cells;[11] receptor for the influenza C virus [gp40/gp36];[12] PA2.26, an antigen induced in epidermal keratinocytes during chemical carcinogenesis and wound healing;[13,14] and platelet aggregation-inducing sialoglycoprotein aggrus).[15] Because PDPN specifically stains lymphatic endothelial cells, it is widely used as a molecular marker for lymphatic vessels and lymphangiogenesis in normal and pathologic tissue samples[16] (for review, see[17,18]). Pdpn-deficient mice die at birth due to respiratory defects.[19] Intriguingly, PDPN has been implicated in malignant progression and invasion of a variety of human cancers, including germ cell carcinoma, tumors of the central nervous system, and squamous cell carcinoma (for reviews see[20,21]). We showed recently that high PDPN protein levels are associated with significantly reduced overall survival among patients with glioma.[22]

Despite the fact that PDPN is highly expressed in many cancer entities, information concerning the regulation of its expression remains largely inconclusive. Recently, we showed a strong induction of Pdpn expression in 2 independent mouse tumor models of skin carcinogenesis and provided experimental evidence that mouse Pdpn is a direct target of the transcription factor Fos, a member of the activator protein-1 (AP-1) protein family.[23–25] Moreover, Noushmehr et al. identified hypermethylation of the PDPN promoter in the G-CIMP subtype of GB,[9] supporting the hypothesis that both genetic and epigenetic modes are implicated in the regulation of PDPN expression.

In this article, we describe a novel mode of PDPN expression in human astrocytic tumors and glioma cell lines through activation of PI3K-AKT-AP-1 signaling. This pathway is under negative control of PTEN, in which activity is often lost in primary GB because of genomic deletion, gene mutation, and epigenetic silencing. Furthermore, we identified a CpG island in the *PDPN* promoter and demonstrated that its hypermethylation is negatively correlated with PDPN expression. In glioma cell lines, demethylation of this site correlated with upregulation of PDPN transcripts, most prominently in the absence of PTEN expression.

Materials and Methods

Human Tumor Samples

A total of 74 astrocytic gliomas were selected from the frozen tumor tissue collections at the Department of Neuropathology, Heinrich-Heine-University, Düsseldorf, Germany; the Department of Neuropathology, Charité Universitätsmedizin, Berlin, Germany; and the International Agency for Research on Cancer, Lyon, France. All tumors were histologically classified according to the criteria of the WHO 2000 classification of tumors of the nervous system, which in the case of astrocytic gliomas, have been retained in the 2007 revised WHO classification.[26] The tumor series consisted of 53 glioblastomas of WHO grade IV, 13 anaplastic astrocytomas of WHO grade III (AAIII), and 8 diffuse astrocytomas of WHO grade II (AII). The glioblastoma group included 42 primary glioblastomas and 11 secondary glioblastomas. Only samples showing a histologically estimated tumor cell content of more than 80% were used for nucleic acid extraction and molecular analysis.

Mice

Mice were housed under standard conditions, and all animal experiments conformed to local and international guidelines for the use of experimental animals. Generation of Tlx-CreER^{T2} mice and the protocol for tamoxifen-induced activation of Cre-recombinase have been described in Liu et al.;[27] mice with the PTEN conditional alleles were obtained from Jackson ImmunoResearch Laboratories. Mice were then perfused with 4% paraformaldehyde 4 weeks after tamoxifen injection, and the brains were postfixed overnight at 4°C; 5-μm paraffin sections were selected for further immunohistochemical (IHC) analysis.

Cell Culture and Transient Transfection of Glioma Cell Lines

All glioma cell lines were cultured in DMEM (PAA) and HEK293T cells in IMEM medium (Invitrogen). Culture medium was supplemented with 10% FCS, 2 mM glutamine (PAA), 100 U/mL penicillin, and 0.1 mg/mL streptomycin (PAA), and the cells were cultured at 37°C in a humidified atmosphere of 8% CO_2 and 21% oxygen (normoxia). Hypoxia was induced by culturing the cells for 72 h in a 37°C humidified atmosphere with 1% oxygen (Incubator C42; Labotect).

LN308 cells were transfected with the different expression plasmids by liposome-mediated transfection

using Lipofectamine2000 (Invitrogen) according to the manufacturer's instructions. Luciferase activities were quantified 18 h after transfection using the Dual Luciferase Assay (Promega). Values were normalized to renilla luciferase activity expressed from pRL-CMV (Promega). The following expression plasmids were used: Pdpn-luci containing the proximal murine Pdpn promoter (−215/+113) in front of the firefly luciferase gene;[24] pcDNA3.1 (Invitrogen); and plasmids encoding wild-type full-length Jun (RSV-Jun), Fos (RSV-Fos), pRC/RSV (RSV-0), dominant negative Jun (dnJun), and Fos (dnFos).[28–32] For generating the 5xTRE-luci construct, the sequence TGAGTCACCAACCTGAC TCAAAGGATTGAGTCAGCAACTT GACTCAAAG GATTGAGTCAAGATCTCTCTGAGCAATAGTATAA AA, comprising 5 consensus AP-1 binding sites in front of a minimal TATA-box sequence,[33] was cloned into the XhoI/HindIII sites of pGL3 (Promega). For cloning the mut5xTRE-luci plasmid, the sequence AGAGT CCCAACCGGACTCTAAGGATAGAGTCCGCAACT GGACTCTAAGGATAGAGTCCAGATCTCTCTGAG CAATAGTATAAAA was inserted into the XhoI/ HindIII sites of pGL3. The 5xTRE-luci and mut5xTRE-luci were kindly provided by M. Schorpp-Kistner (German Cancer Research Center); BCGH-PTEN encoding full-length human PTEN was kindly provided by H. Zentgraf (German Cancer Research Center).

Nucleic Acid Preparation

DNA and RNA for array-CGH and expression profiling were prepared from freshly frozen tumor tissue as reported previously.[34,35] Genomic DNA of U87MG and LN18 cells was extracted using the DNeasy Blood and Tissue Kit (Qiagen); total RNA from cell lines was prepared using the peqGOLD TriFast (Peqlab Biotechnologie) or RNeasy Mini Kit (Qiagen) according to the manufacturer's instructions. Quality and quantity of the nucleic acid samples were determined using a NanoDrop spectrophotometer (NanoDrop Technologies).

Array-CGH and Expression Profiling

Array-CGH and gene expression profiling were performed as previously reported.[5] Data were analyzed using EnsEMBL (version 51) with packages of the Bioconductor project[36] implemented in our in-house–developed ChipYard framework for microarray data analysis (http://www.dkfz.de/genetics/ChipYard/) and deposited in the NCBI Gene Expression Omnibus (GEO) database (accession no. GSE15698510).

Real-time Quantitative Polymerase Chain Reaction (RQ-PCR)

RNA was reverse transcribed as described.[37] RQ-PCR was performed using the MyiQ Single-Color Real-Time PCR Detection System (Bio-Rad) according to the manufacturer's instructions. The Absolute SYBR Green Fluorescein Kit (ABgene) was used according to the manufacturer's instructions. All RQ-PCR experiments were performed in triplicate and normalized onto *LaminB1*. Sequences of the primers used were *hPDPN* forward: 5′TTCATTGGTGCAATCATCGT 3′; *hPDPN* reverse: 5′AGAGGAGCCAAGTCTGG TGA 3′; *LaminB1* forward: 5′CTGGAAATGTTTGC ATCGAAGA 3′; and *LaminB1* reverse: 5′GCCTCCCA TTGGTGGATCC 3′.

Bisulfite Treatment and Methylation Analysis

For each specimen, 1–2 μg of genomic DNA was treated with sodium bisulfite using the EpiTect Bisulfite Kit (Qiagen). For analysis, a CpG island in the *PDPN* 5′-region was chosen using the UCSC Genome Browser (http://genome.ucsc.edu) defining CpG-islands by the following criteria: GC content >55%, length >200 bp, and observed CpG/expected CpG ratio of >0.6. DNA primers (forward: 5′-GCGGCCGCGTT GTTGAGTAGAATAAAAGTTTATTTTGTTAGG-3′; reverse: 5′-CAACAAACTTTACAATTAAAAACTT TC-3′) were designed specifically amplifying bisulfite-converted DNA and generating amplicons in the island (chr1:13910138-13910868). Methylation analysis covered 20 of 59 CpG sites of this island. PCR amplicons were purified from agarose gels with use of the Rapid Gel Extraction System (Marligen Biosciences). Sequencing reactions were conducted using BigDye Terminator 3.1 (Applied Biosystems) according to the manufacturer's recommendations and were analyzed on a fully automated ABI PRISM 3100 genetic analyzer (Applied Biosystems) using the primer 5′-CA ACAAACTTTACAATTAAAAACTTTC-3′. For each CpG, the methylation status was rated on a scale ranging from 0 (not methylated) to 3 (strongly methylated) according to the methylated-to-unmethylated signal ratios (0, unmethylated signal only; 1, ratio <1:3; 2, ratio 1:3–2:3; 3, ratio >2:3). For a positive control, we applied enzymatically methylated human male genomic leukocyte DNA that was modified using CpG methyltransferase *M.Sss* (New England Biolabs) according to the manufacturer's protocol. The promoter was scored as methylated when methylation was detected at ≥50% of the CpG dinucleotides.

Histochemical and Immunostaining Analyses

IHC analysis on paraffin sections was performed using biotinylated secondary antibodies and the Vectastain Elite ABC kit (Vector Laboratories). Double IHC staining was performed using the ImmPRESS anti-rabbit Ig peroxidase polymer detection kit (Vector Laboratories) and the IHC-Kit DCS SuperVision RED (mouse/rabbit) 2 Polymer-AP-detection system (DCS) according to the manufacturers' instructions. For substrates, we used liquid AEC+ Substrate Chromogen (Dako) or VectorRed and Histogreen (Vector Laboratories). Sections were counterstained with hematoxylin and/or eosin as indicated. All antibodies used are listed in Table 1.

Table 1. Antibodies used for immunohistochemistry and Western blot analyses

Name	Species	Number	Assay	Company
Primary antibodies				
Human PDPN	Mouse	D2-40	IHC, WB	Covance, Princeton, NJ, USA
Mouse PDPN	Syrian hamster	8.1.1	IHC	Developmental Studies Hybridoma Bank, University of Iowa, Iowa City, IA, USA
c-Fos	Rabbit	sc-7202	IHC	Santa Cruz Biotechnology, Santa Cruz, CA, USA
c-Jun	Rabbit	ab32137	IHC	Abcam, Cambridge, UK
Phospho-Akt (Ser473)	Rabbit	4058	WB	Cell Signaling Technology, Boston, MA, USA
Total Akt	Rabbit	9272	WB	Cell Signaling Technology
Phospho-ERK1/2 (12D4)	Mouse	sc-81492	WB	Santa Cruz Biotechnology
Total ERK(K23)	Rabbit	sc-153	WB	Santa Cruz Biotechnology
β-Actin (AC-15)	Mouse	A5441	WB	Sigma-Aldrich, Munich, Germany
Secondary antibodies				
Anti-Syrian hamster biotin-SP-conjugated			IHC	Jackson ImmunoResearch Laboratories, West Grove, PA, USA
Biotinylated anti-rabbit IgG			IHC	Vector Laboratories, Burlingame, CA, USA
Anti-mouse IgG, HRP-linked antibody			WB	Cell Signaling Technology
Anti-rabbit IgG, HRP-linked antibody			WB	Cell Signaling Technology
ImmPRESS anti-rabbit Ig peroxidase polymer detection kit		MP-7401	IHC	Vector Laboratories
IHC-Kit DCS SuperVision RED 2 Polymer-AP-detection system (mouse/rabbit)		AD000POL	IHC	DCS, Hamburg, Germany

Abbreviations: IHC, immunohistochemistry; WB, Western blot.

Western Blot Analysis

Protein isolation and Western blot analysis were performed as described previously.[38] Primary and secondary antibodies used are listed in Table 1. Quantification was performed using the ImageJ program.

5-Aza-2′-Deoxycytidine and Trichostatin A Treatment

Cells were incubated for 72 h with 5′-aza-2′-deoxycytidine (5-aza-dC; 500 nM; Sigma-Aldrich) with the culture medium being replaced every 24 h with fresh medium containing 5-aza-dC. In the case of combination with trichostatin A (TSA; 1 μM; Sigma), this drug was added for the last 24 h of the 5-aza-dC treatment. Phosphate-buffered saline (PBS) was used as the dissolvent control.

PDPN Silencing

Lentiviral particles were produced using transient cotransfection of podoplanin MISSION shRNA vectors, purchased from Sigma-Aldrich (see below), with pMDLg-pRRE and pRSV-REV packaging vectors, and the pMD2-VSVG envelope vector in HEK293T cells. These vectors were kindly provided by Dr. Luigi Naldini (San Raffaele Telethon Institute for Gene Therapy, University Medical School, Milan, Italy). Sequences and TRC numbers of the PDPN shRNAs were as follows: sh1: TRCN0000061924, 5′CCGGGCTATAAGTCTGGCTTGACAACTCGAGT TGTCAAGCCAGACTTAT AGCTTTTTG 3′; sh2: TRCN0000061927; 5′CCGGGCAACAAGTGTCAA CAGTGTACTCGAGTACACTGTTGACACTTGT TG CTTTTTG3′; sh3 (nonfunctional): TRCN0000061925; 5′CCGGCGGCTTCATTGGTGCAATCATCTCGAGA TGATT GCACCAATGAAGCCGTTTTTG3′; nontarget (scrambled shRNA): catalogue #SHC002V.

For the transfection of 1 dish, 12.5 μg of pMDLg-pRRE plasmid, 6.25 μg of pRSV-REV, 9 μg of pMD2-VSVG, and 32 μg of shRNA vector were mixed in 1 mL of OPTIMEM medium containing 179.25 μg/mL polyethylenimine. After 30 min of incubation at room temperature, the transfection mixture was added to the cells. Twenty-four hours after transfection, the virus was purified by ultra-centrifugation for 2 h at 20°C.

For lentiviral transduction, 1×10^4 LN308 cells were seeded onto a 48-well plate and transduced with lentiviral particles; transduced cells were selected with puromycin (0.5 μg/mL).

Cell Proliferation Assay

The cell proliferation assay was performed using the APC BrdU Flow Kit (BD Biosciences) according to the manufacturer's instructions.

Migration Assay

LN308 cells with PDPN knock-down (LN308 PDPN sh1, LN308 PDPN sh2), and control cells (LN308 nontarget, LN308 with nonfunctional sh3) were seeded on

both sides of IBIDI cell culture inserts (25,000 cells per side; catalogue #80209; IBIDI) and cultured for 24 h to reach confluency. Cells were treated with 10 μg/mL mitomycin C (Sigma) for 1 h and washed intensively with PBS. The inserts were subsequently removed. Images were taken at the indicated time points using light microscopy and a digital camera (Olympus). The distance between the migration fronts was measured using the UTHSCSA Image tool software (http://ddsdx.uthscsa.edu/dig/itdesc.html).

Statistical Analysis

Statistical analyses and graphics were performed using R or Microsoft Excel software. Standard deviation (SD) is indicated by error bars; $P < .05$ was considered to be statistically significant.

Results

Coexpression of PDPN and AP-1 Family Members in Primary GB

We demonstrated recently, using a small set of tumor samples from patients with glioma ($n = 20$), that PDPN transcripts are highly abundant in primary GB but show no or very weak expression in lower-grade astrocytoma or secondary GB.[22] This association was further confirmed in the current study by detailed analysis of global gene expression profiling data of a larger cohort of tumors ($n = 74$). Consistent with our previous findings, PDPN transcript levels were significantly upregulated in primary GB, compared with secondary GB or lower-grade astrocytoma ($P < .001$) (Fig. 1A).

To define the molecular mechanism of PDPN regulation in primary GB, we determined transcript levels of the transcription factor activator protein 1 (AP-1) family members JUN and FOS, which were shown recently to drive PDPN expression in mouse models of skin carcinogenesis.[24,25]

Indeed, analysis of expression profiling data for FOS and JUN transcript levels on glioma tumor samples paralleled expression of the PDPN transcript with the highest expression in primary glioblastoma (Fig. 1A). The heatmap in Fig. 1B illustrates the correlation of PDPN, JUN, and FOS expression levels in the individual tumor samples (PDPN-JUN: Pearson correlation 0.6686043, Spearman rank correlation 0.660208; PDPN-FOS: Pearson correlation 0.42475646, Spearman rank correlation 0.428839; JUN-FOS: Pearson correlation 0.61113774, Spearman rank correlation 0.643112). Coexpression of JUN and FOS proteins with PDPN was further corroborated by IHC staining of tumor sections from human GB. We found the most intense PDPN immunoreactivity (IR) adjacent to necrotic areas in the palisading cells that most likely represent poorly differentiated cells, which are migrating from the necrotic area because of a hypoxia-induced gradient of tissue oxygen concentration.[39] Consistent with the assumption that PDPN is a direct target of AP-1, FOS and JUN proteins were detected in areas with high PDPN IR (Fig. 1C). Coimmunostainings for PDPN and JUN/FOS are depicted in Supplementary material, Fig. S1. In line with the regulatory function of AP-1 activity in PDPN expression, most JUN IR-positive cells in perinecrotic tumor cells express PDPN protein, whereas FOS protein is more widely expressed, in corroboration with our previous observations in chemically induced mouse skin tumors.[24]

Regulation of PDPN Expression by the PI3K-AKT-AP-1 Signaling Pathway

To further confirm the functional involvement of AP-1 in regulation of PDPN expression, we transiently cotransfected the PDPN-positive cell line LN308 with a construct containing the proximal murine *Pdpn* promoter (−215/+113) in front of the firefly luciferase gene (mPdpn-luci[24]) and expression plasmids encoding dominant-negative mutants of Jun or Fos proteins, respectively. Ectopic expression of dominant-negative versions of Jun and Fos proteins resulted in significant downregulation of basal *Pdpn*-promoter–driven luciferase activity (Fig. 2A). Vice versa, overexpression of wild-type Jun and Fos proteins resulted in a small but significant increase of reporter genes driven by the *Pdpn*-promoter (Fig. 2B) or an artificial AP1-dependent promoter comprising five consensus AP-1 binding sites (5xTRE-luci; Fig. 2C). The minor effects (1.7-fold and 3-fold, respectively) on both reporters are likely attributable to high basal AP-1 activity in LN308 cells, as indicated by the 100-fold difference in expression of reporters containing either the wild-type or the mutant version (mut 5xTRE-luci) of the TRE sequence (Fig. 2C). Taken together, these results support the crucial role of AP-1–mediated transcriptional activation of PDPN expression in glioma cells. Putative upstream signaling pathways of AP-1 in glioma comprise the mitogen-activated protein kinase/extracellular signal regulated kinase (MAPK/ERK)[40] and the phosphatidylinositol-3 kinase (PI3K) pathway.[41] To analyze the involvement of these pathways in the regulation of PDPN expression, we treated LN308 and U87MG cells with 2.5 μM of the PI3K inhibitor LY294002, 10 μM of the MAPK/ERK pathway inhibitor UO126, or both. Treatment with LY294002 resulted in a strong decrease in PDPN protein levels, whereas treatment with UO126 had no effect. Accordingly, the combination of both inhibitors did not further decrease PDPN protein levels (Fig. 2D and Supplementary material, Fig. S2), implying that AP-1–mediated PDPN expression in glioma cells is downstream of PI3K activation.

Inverse Correlation Between PDPN and PTEN Expression in Glioma Samples and a Pten-deficient Mouse Model

Deregulation of the PI3K-AKT pathway, one of the most important features of glioma progression, is often

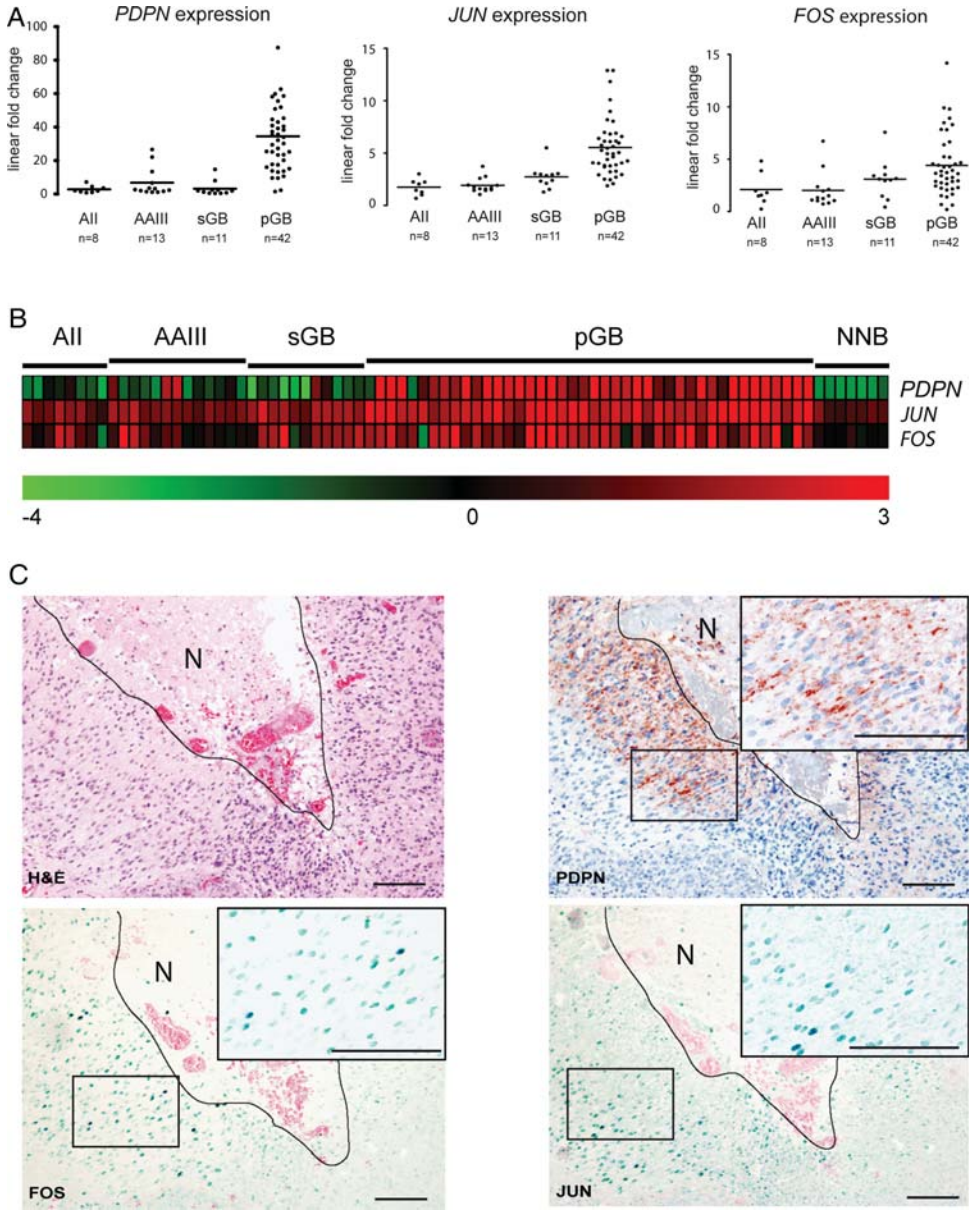

Fig. 1. (A) PDPN mRNA expression is significantly higher in primary glioblastoma grade IV (pGB) than in lower-grade astrocytoma (AII, AIII) or secondary glioblastoma (sGB; $P < .001$, t test). FOS and JUN transcript levels in different stages of astrocytoma correlate with the expression pattern of PDPN and similarly show the highest expression in pGB. Single dots indicate the individual PDPN, FOS, and JUN expressions normalized to the mean expression in 7 normal brain samples. Median expression is indicated by horizontal lines. (B) Heatmap depicting the relative PDPN, JUN, and FOS expression levels in the individual tumor samples. Abbreviations in (A) and (B): AII, astrocytoma WHO grade II; AAIII, anaplastic astrocytoma WHO grade III; sGB, secondary glioblastoma; pGB, primary glioblastoma; NNB, nonneoplastic (healthy) brain. (C) Sections of formalin-fixed, paraffin-embedded samples of human glioblastoma were analyzed by immunohistochemical staining with antibodies against PDPN (red, upper right panel), FOS (green, lower left panel), and JUN protein (green, lower right panel). PDPN immunoreactivity is present in perinecrotic cells and overlaps with FOS and JUN protein expression. Scale bars: 200 μm. Small boxes show higher magnifications of the indicated immunoreactive areas (scale bars: 100 μm). Cellular morphology of the sections was visualized by H&E staining (upper left panel). N = necrotic area.

provoked by loss or inactivation of its upstream negative regulator PTEN (for recent reviews see [42,43]). Indeed, we found that monoallelic PTEN loss significantly correlated with high PDPN transcript levels in human GB samples (41 of 50; $P \leq .001$, Fisher's exact test). In lower-grade tumors, samples with biallelic PTEN retention exhibited low PDPN transcript levels in most cases (15 of 21). Throughout all analyzed samples ($n = 69$), *PTEN* and *PDPN* transcript levels were inversely correlated (Spearman rank correlation = −0.446; $P < .001$; and Kendall tau rank correlation = −0.305, $P < .001$). An inverse relationship between *PTEN* and *PDPN* transcript

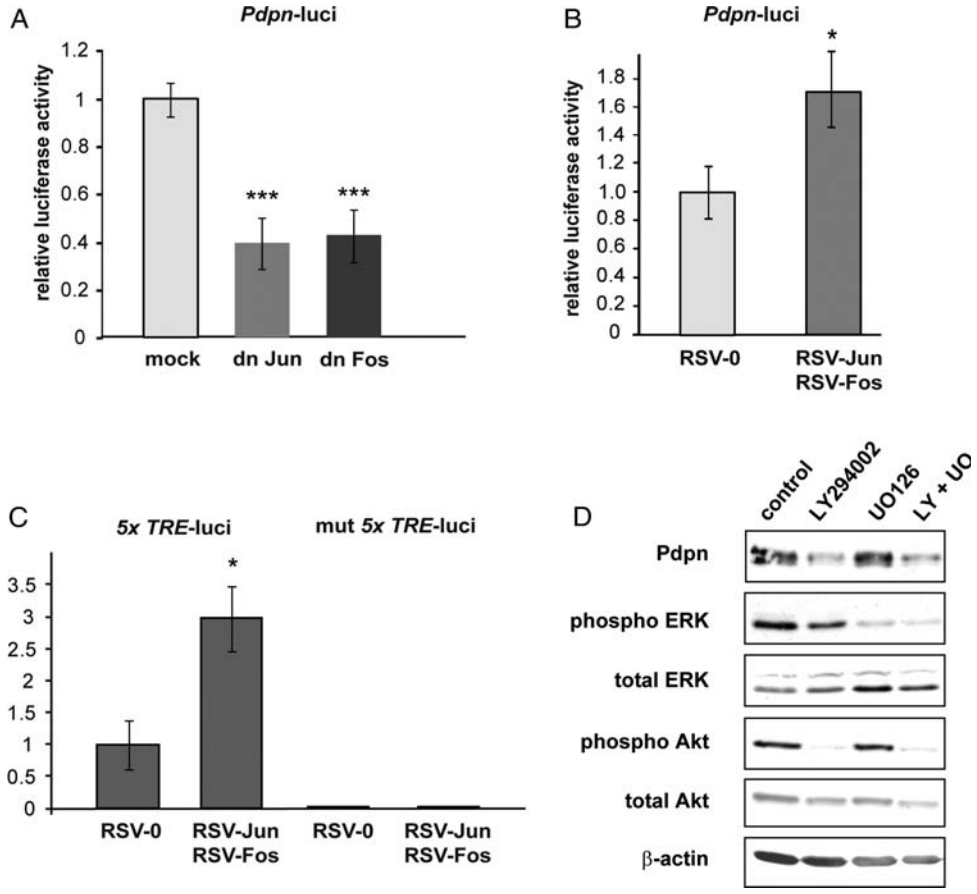

Fig. 2. PDPN expression is regulated by AP-1 and the PI3K pathway in glioma cells. (A) Dominant-negative Fos and Jun mutants interfere with basal activation of the mouse *Pdpn* promoter in LN308 cells. Cells were cotransfected with a luciferase reporter plasmid under the control of the *Pdpn*-promoter (*Pdpn*-luci) and an empty plasmid (mock) or dominant-negative Jun (dn Jun) or Fos (dn Fos) expression plasmids. Luciferase activity was measured 18 h after transfection. The bars represent means and standard deviation of 4 experiments with all conditions performed in triplicate. $***P < .001$. (B) Expression of wild-type Jun and Fos increases PDPN-luci activity. LN308 cells were cotransfected with *Pdpn*-luci and empty vector (RSV-0) or plasmids encoding full-length Jun (RSV-Jun) and Fos (RSV-Fos). Luciferase activity was measured 18 h after transfection. The bars represent means and standard deviation of 3 experiments with all conditions performed in triplicate. $*P < .05$. (C) The artificial AP-1 reporter 5xTRE-luci, but not its mutant version, is activated by coexpression of Jun and Fos. LN308 cells were cotransfected with 5xTRE-luci or 5xmutTRE-luci and RSV-0 or RSV-Jun RSV-Fos. Luciferase activity was measured 18 h after transfection. The bars represent means and standard deviation of 3 experiments with all conditions performed in triplicate. $***P < .001$. (D) Western blot analysis of PDPN protein levels in LN308 cells after 24 h of treatment with the PI3K inhibitor LY294002, the ERK cascade inhibitor UO126, or both, compared with control. Note that in the presence of LY294002 PDPN levels are significantly reduced, whereas UO126 has no effect. The extracts were reprobed with antibodies against phospho-Akt, total Akt, phospho-ERK, and total ERK to show efficacy of the inhibitors. β-Actin protein detection served as a control for equal loading of proteins.

abundance was also observed in tumors in which *PTEN* was retained ($n = 23$), although the correlation did not reach statistical significance (Spearman rank correlation = −0.330, $P = .122$; and Kendall tau rank correlation = −0.233, $P = .125$). Taken together, these findings suggest a possible direct or indirect negative effect of PTEN function on PDPN expression in glioma cells.

To confirm the causal relationship between loss of PTEN activity and increased PDPN expression in an in vivo model, we used mice with conditional inactivation of Pten in neural stem cells. These were obtained by crossing mice with tamoxifen-inducible expression of the Cre-recombinase under control of the orphan nuclear receptor tailless (Tlx)–promoter with mice bearing the floxed allele of Pten.[27]

Immunostaining in wild-type mice revealed prominent Pdpn protein expression in the ependymal layer of the lateral ventricles. In agreement with the inverse correlation of PTEN and PDPN expression in human primary GB samples, $Pten^{NSC-/-}$ mice exhibited strong Pdpn protein expression, which was extended to the subventricular zone (SVZ) and the rostral migratory stream. These data strongly support a negative regulatory effect of Pten on Pdpn expression in SVZ neural stem/progenitors in vivo (Fig. 3).

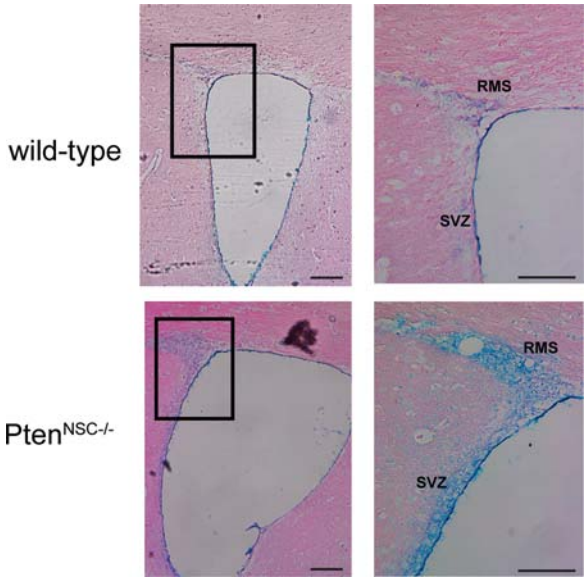

Fig. 3. PDPN expression is inversely correlated with the presence of functional PTEN: comparison between Pdpn protein expression in the subventricular zone (SVZ) and rostral migratory stream (RMS) of wild-type and $Pten^{NSC-/-}$ mice. Panels show immunohistochemical staining for mouse Pdpn (green); counterstaining was performed with eosin (scale bars: 200 μm). Right panels show higher magnifications (scale bars: 100 μm) of the indicated areas. Note that $Pten^{NSC-/-}$ mice exhibit increased Pdpn immunoreactivity in the SVZ and RMS.

PTEN Negatively Regulates PDPN Expression in Human Glioma Cell Lines

To analyze the role of PTEN in the regulation of PDPN expression in more detail, we made use of 7 established human glioma cell lines with known PTEN status.[44] As depicted in Fig. 4A, cell lines with wild-type PTEN (LN18, LN229T, and LN428) were negative for PDPN both on the mRNA and protein level, whereas cell lines with mutant (inactive) PTEN (LN308, LN319, U87MG, and U373MG) exhibited robust PDPN mRNA and protein expression. Next, we reconstituted PTEN function in LN308 cells that harbor a functional loss of PTEN protein due to a missense mutation in the *PTEN* gene, by transient transfection with a human PTEN expression plasmid. Reconstitution of PTEN function resulted in a strong decrease of AKT kinase phosphorylation accompanied by a marked reduction of PDPN protein levels (Fig. 4B). In line with the negative effect of PTEN re-expression on PDPN protein expression in LN308 cells, coexpression of the PTEN expression plasmid with mPdpn-luci revealed a significant downregulation of promoter activity, supporting direct inhibition of PDPN transcription upon activation of PTEN (Fig. 4C).

Effect of Hypoxia on the Expression of PDPN in Glioma Cells

PDPN staining was most prominent in the perinecrotic areas in human GB tumors, which comprise hypoxic niches with a key role in tumor progression. To analyze whether hypoxic conditions affect PDPN expression, we compared PDPN transcript levels in the PTEN-negative glioma cell lines LN308 and U87MG and the PTEN–wild-type cell line LN428 under normoxic and hypoxic conditions. In the LN308 and U87MG cells, 72 h of hypoxia resulted in a robust increase of PDPN mRNA, compared with normoxic expression levels, consistent with recent observations in U87MG cells.[45] There was no effect on LN428 cells, indicating that the presence of functional PTEN prevented induction of PDPN in these cells (Fig. 4D).

Regulation of Pdpn Expression in Human GB by Promoter Methylation

In addition to genetic mechanisms, epigenetic regulation, primarily differential promoter methylation, has been proven to be an important means of modifying gene expression during development and tumorigenesis (for recent reviews, see [46,47]). Of interest, in a recently described G-CIMP phenotype, PDPN represented one of the top candidate genes, whose expression was most likely regulated by promoter methylation.[9] Strikingly, in some of our secondary glioblastoma samples, PDPN transcript levels were low or even absent despite the occurrence of mutated PTEN. To investigate alterations in promoter methylation in glioblastoma samples, we focused on a CpG island located in the 5′ upstream region of the human *PDPN* gene (UCSC Genome Browser on Human Feb. 2009 (GRCh37/hg19) assembly – chr1:13,906,833–13,941,031). This CpG island, located at chromosome 1:13,910,138–13,910,868 and including the nucleotide sequence −114 to +1, exon 1 (343 nt) and 274 nt of intron 1, contains 59 CpGs. Twenty of them, covering 5′ upstream sequences and the start site of transcription (−114 to +86), were analyzed by bisulfite sequencing (CpG number 1–20 in Fig. 5A). Primary GB samples showed low or absent methylation of this CpG island, consistent with the expression of PDPN and the mono- or biallelic loss of PTEN (PTEN status: −1, −2). In most of the secondary GB, the CpG island was hypermethylated, consistent with the lack of PDPN expression. In the few cases of secondary GB, which showed monoallelic loss of PTEN and low expression of PDPN, methylation of the CpG island was considerably lower (cases no. 18, 20, and 25 in Fig. 5A). In contrast, in nonneoplastic brain tissue (NNB), the CpG island was completely unmethylated; however, PDPN was not expressed, presumably because of the negative regulation by wild-type PTEN. This analysis suggested a negative correlation between promoter hypermethylation and PDPN transcript levels, which was confirmed by statistical analysis as shown in Fig. 5B (2-sample exact Wilcoxon test, $P < .001$).

To further test this assumption, we compared the methylation status with PDPN transcript levels in the presence and absence of the demethylating agent 5-aza-2′-deoxycytidine (5-aza-dC) with or without the

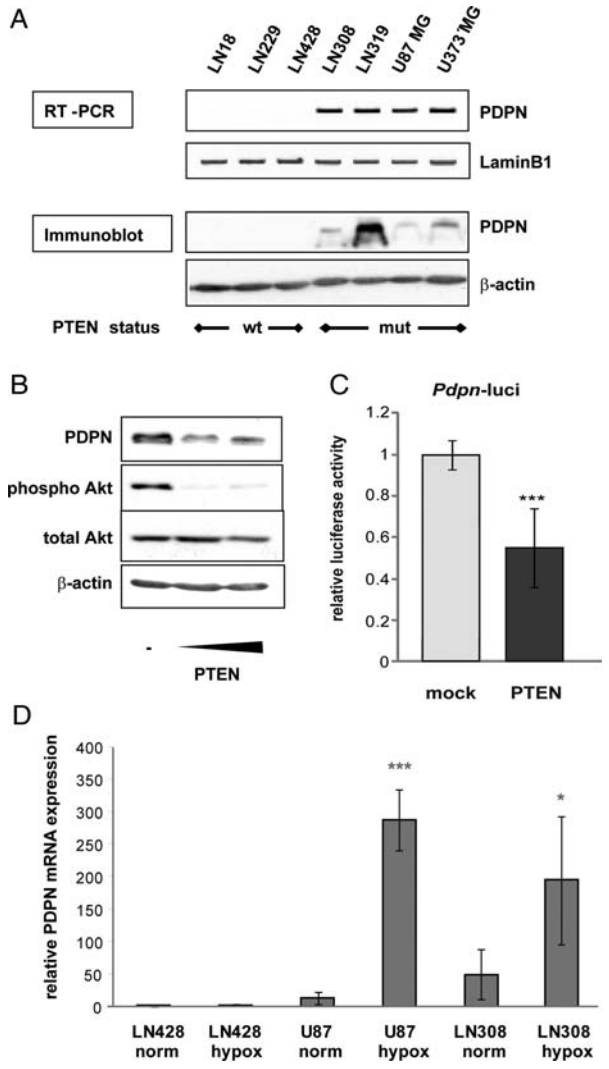

Fig. 4. Reduced PDPN expression by PTEN is mediated by the PI3K pathway. (A) PDPN expression was analyzed on transcript (RT-PCR) and protein levels (immunoblot) in 7 human glioblastoma cell lines with wild-type (wt) or mutant (mut) PTEN. Cell lines harboring mutations in PTEN show PDPN transcript and protein expression and vice versa. LaminB1 transcript levels served as control for cDNA quality and quantity, and β-actin protein detection served as a control for equal loading of proteins. (B) Ectopic expression of wild-type PTEN in LN308 cells harboring a PTEN mutation results in reduced PDPN protein expression and a decrease in Akt phosphorylation. LN308 cells were transfected with increasing amounts of expression vector encoding wild-type PTEN. Whole-cell lysates were prepared 24 h after transfection and analyzed by immunoblots for the indicated proteins. β-Actin protein detection served as a control for equal loading of proteins. (C) Ectopic PTEN expression inhibits luciferase reporter gene activity under the control of the proximal mouse *Pdpn* promoter. LN308 cells were cotransfected with a *Pdpn*-promoter luciferase reporter (Pdpn-luci) and empty vector (mock) or an expression plasmid for wild-type PTEN; luciferase activity was measured 18 h after transfection. The bars represent means and standard deviation of 4 experiments with all conditions performed in triplicate. $***P < .001$. (D) PDPN expression is induced under hypoxic conditions in U87MG and LN308 cells with mutant PTEN but not in L428 cells (PTEN wild-type). Enhanced *PDPN* transcript levels in hypoxic cells (hypox) are indicated as fold difference compared with the expression in normoxic LN428 cells (normox). Error bars show SD values of at least 4 independent experiments. $*P < .05$, $***P < .001$.

histone deacetylase inhibitor TSA in 2 glioma cell lines: LN428 cells (PTEN wild-type, PDPN negative) and U87MG cells with mutant PTEN and moderate expression of PDPN (see Fig. 4A). As depicted in Fig. 5C, treatment of U87MG cells with 5-aza-dC resulted in an almost 3-fold increase in PDPN transcript levels, which was further increased to 6-fold over basal levels in the presence of TSA. In contrast, PDPN mRNA remained almost undetectable in LN428 cells, although in both cell lines, methylation of the PDPN promoter CpG island was reduced (Fig. 5D). This lack of induction of PDPN expression in LN428 cells, similar to the absence of hypoxia-driven enhancement of PDPN transcript levels in these cells, is most likely attributable to the presence of functional PTEN.

Reduced Cell Proliferation and Migration in PDPN-Compromised LN308 Glioma Cells

There is increasing evidence that the level of PDPN expression is correlated with higher tumor malignancy in human patients and in mouse tumor models (for reviews see [20,21]). To test the functional role of PDPN expression, we silenced PDPN expression in LN308 glioma cells using a lentiviral shRNA strategy. Efficient downregulation of PDPN protein abundance by shRNA 1 and 2 (PDPN sh1, PDPN sh2) was confirmed by Western blot (Fig. 6A, about 80% for PDPN sh1 and 96% for PDPN sh2). In contrast, LN308 cells infected with shRNA 3 (nonfunctional sh3) or a scrambled shRNA (nontarget) showed comparable protein levels and were used as controls for further experiments. As depicted in Fig. 6B and C, silencing of PDPN resulted in impaired cell proliferation and migration of LN308 cells. Taken together, these analyses further support an important functional role of PDPN in the progression and malignancy of GB.

Discussion

Previously, Phillips et al.[6] proposed a classification of brain tumors by genetic profiles attributed to a proneural, mesenchymal, or proliferative phenotype, whereby the 2 latter comprise most of the high-malignant WHO grade III anaplastic astrocytoma and WHO grade IV GB. In this study, PDPN was one of the genes showing specific overexpression in the mesenchymal molecular subclass of high-grade astrocytoma, a signature that resembles that of neural stem cells.[6] In a recently developed advanced classification of GB signatures, comprising proneural, neural, classical, and mes-

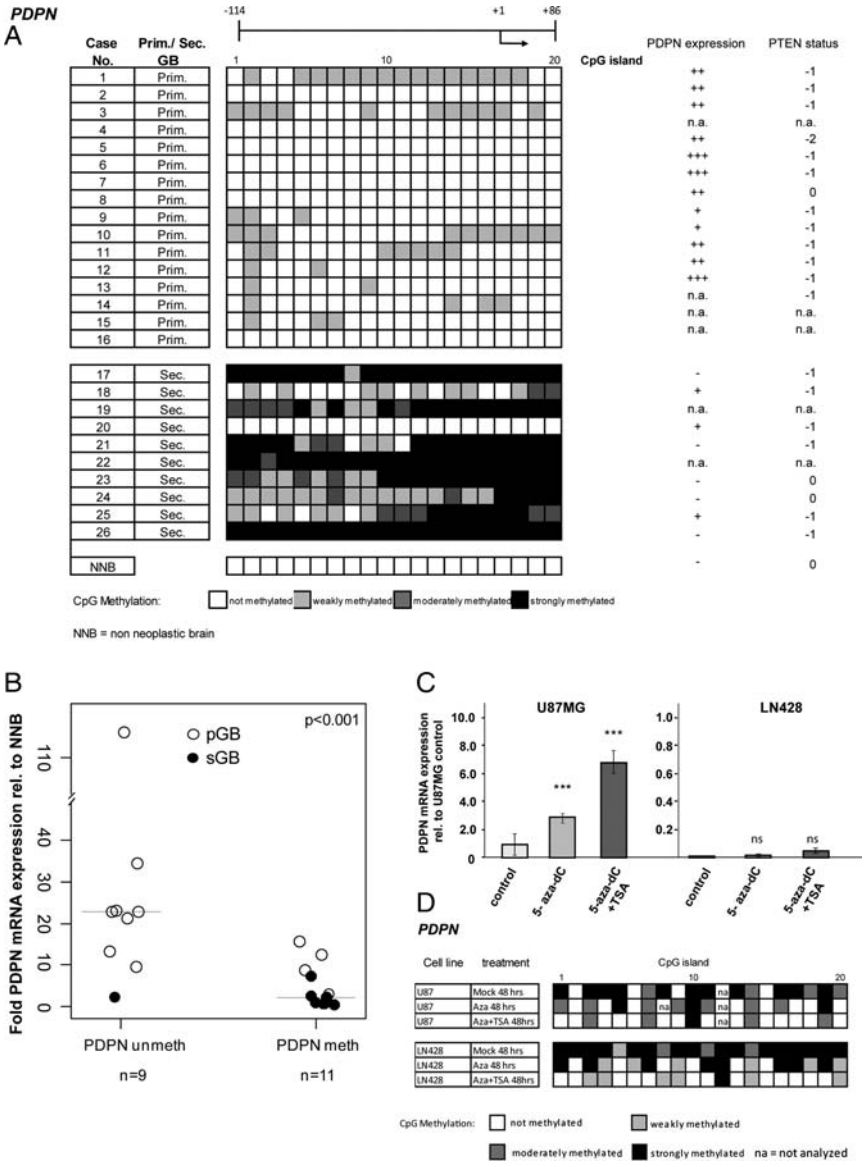

Fig. 5. Epigenetic regulation of PDPN expression in human glioma samples and glioma cell lines. (A) Genomic DNA from frozen tumor tissues of primary and secondary glioblastoma and normal brain was used for bisulfite sequencing of a CpG island in the *PDPN* 5′-region. For each CpG-dinucleotide, the methylation status was rated according to the following scale: 0, not methylated (white square); 1, weakly methylated (ratio peak area of unmethylated signal/methylated signal $<1/3$; light grey square); 2, moderately methylated (ratio peak area of unmethylated signal/methylated signal between 1/3 and 2/3; dark grey square); 3, strongly methylated (black square) (ratio peak area of unmethylated signal/methylated $>2/3$). Whereas all secondary glioblastomas were at least moderately methylated, only 9 (56%) of 16 of the primary glioblastoma samples showed weak methylation. PDPN expression in the tumor samples is depicted in comparison to the expression in nonneoplastic brain (NNB), with $++$: $>$30-fold vs. NNB; $++$: $>$10-fold vs. NNB; $+$: $>$ 2-fold vs. NNB, $-$: $<$2-fold vs. NNB; n.a.: not analyzed. The PTEN status is depicted as follows: 0, both PTEN alleles are present; −1, monoallelic loss; −2, biallelic loss of PTEN; n.a., not analyzed. (B) PDPN transcript levels are inversely correlated to the methylation status of the *PDPN* promoter region. Scatter plot depicting fold PDPN transcript levels relative to nonneoplastic brain. GB samples exhibiting PDPN promoter hypermethylation (PDPN meth) in the CpG island depicted in (A) compared with samples with unmethylated PDPN-promoter (PDPN unmeth). Primary glioblastomas (pGB) are depicted with open circles and secondary glioblastomas (sGB) with filled circles. (C) Increase in PDPN transcript levels by demethylating agents in PTEN-negative U87MG cells, but not in LN428 cells with wild-type PTEN. U87MG and LN18 cells were treated for 72 h with 5-aza-dC (500 nM) with or without TSA (1 μM, last 24 h of 5-aza-dC treatment) or with vehicle alone (control). RQ-PCR was performed with primers specific for human PDPN and normalized to LaminB1 transcript levels. PDPN transcript levels of U87MG control were set to 1. Bars show mean and standard deviation of triplicate measurements for each of 3 independent experiments. $***P < .001$, $**P < .01$; n.s., not significant. (D) The glioma cell lines LN428 and U87 were treated as described in (C). Genomic DNA was used for analysis of methylation of the CpG island in the *PDPN* promoter according to (A). Note the decrease in methylation upon treatment with 5′-aza-2′-deoxycytidine (5-aza-dC) in the presence and absence of trichostatin A (TSA).

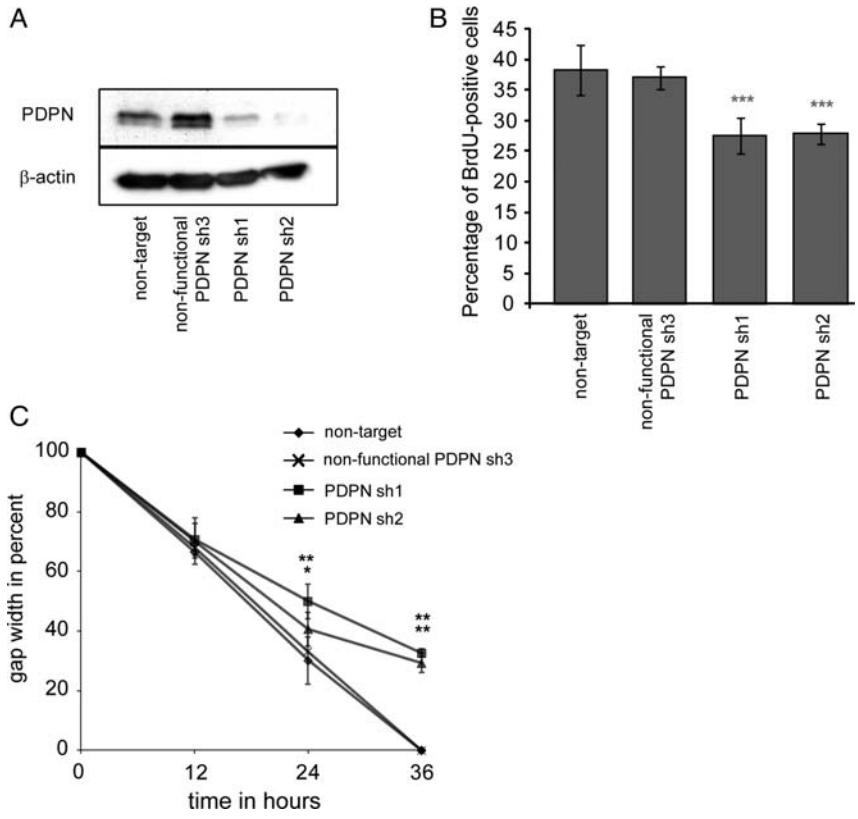

Fig. 6. PDPN silencing impairs proliferation and migration of LN308 glioma cells. (A) Western blot analyses with extracts from LN308 cells transduced with PDPN shRNAs 1-3 and scrambled (nontarget) control. Transduction with PDPN sh1 and sh2 resulted in downregulation of PDPN protein compared with nontarget and PDPN shRNA3 (nonfunctional) transduced LN308 cells. (B) Proliferation of LN308 is significantly reduced in the presence of PDPN sh1 and sh2. The percentage of BrdU-positive cells was determined by FACS analysis. The bars represent means and standard deviation of 4 experiments with all conditions performed in triplicate $***P < .001$. (C) Downregulation of PDPN expression results in slower migration of LN308 cells. LN308 cells transduced with the indicated shRNA constructs were seeded in a migration chamber with a defined gap width. Gap closure was followed over a period of 36 h. The experiment was performed 4 times with each cell line tested in quadruplicate per assay. $*P < .05$, $**P < .01$.

enchymal subtypes, PDPN clustered with genes in the mesenchymal signature exhibiting the second highest expression in the classical signature but was mostly absent in the neural or proneural signature.[7] Moreover, most of the genes that are coregulated with PDPN in our tumor samples are present in either the classical or the mesenchymal signature published by Verhaak et al.[7] (data not shown). This is in concordance with the fact that the mesenchymal and the classical signatures are characterized by loss/mutation of PTEN and higher activity of the PI3kinase/Akt pathway, compared with the proneural signature.[48,49] Accordingly, we found PDPN to be regulated by the PI3K/AKT pathway in glioma cell lines. Upstream of PI3K/AKT, we identified PTEN as a negative regulator of PDPN expression. It has been shown previously that PTEN regulates the transcription factor AP-1 by decreasing the expression of FOS and that PI3K plays a crucial role in FOS expression in the glioma cell line U87MG.[41] Our finding that PDPN expression is regulated by AP-1 is in line with our previous findings that identified PDPN as a direct Fos target gene in a mouse model of skin tumorigenesis.[24]

Genes encoding components of the PI3K/PTEN signaling pathway are among the most frequently mutated genes in cancer, and thus, aberrant PI3K signaling is a key feature of human tumorigenesis and tumor progression (for a recent review, see [50]). Of note, the PTEN status of tumors from patients with GB determined the ability of the tumor cells to grow as neurosphere cultures.[51] It has been postulated that PDPN might be a potent marker for tumor-initiating cells in skin cancer,[52] and there is increasing evidence that this may also hold true for brain tumors.[4,22] Because we found high PDPN expression in glioma tumor neurospheres,[22] it is tempting to speculate that the PI3K-AKT-AP-1-PDPN signaling pathway may be involved in tumor progression from tumor-initiating cells.

Therapeutics targeting PI3K or its downstream kinase AKT have emerged as potential treatment strategies for cancer patients in preclinical studies on different cancer entities (for reviews, see [53–55]). Our finding that PDPN is a downstream target of PI3K suggests the usability of downregulation of PDPN expression as an indicator of successful interference with this pathway.

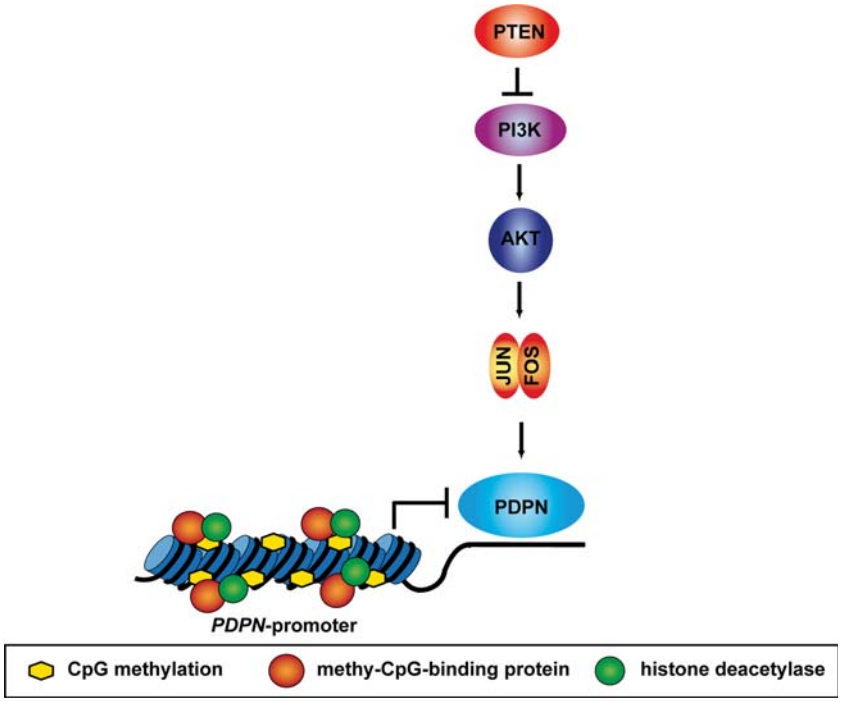

Fig. 7. PDPN expression in gliomas is regulated by a PTEN-PI3K-AP-1 axis and promoter methylation.

We found that, in vitro, silencing PDPN expression leads to reduced proliferation and migration of glioblastoma cells (Fig. 6) and causes diminished cell invasion of glioblastoma spheroids in 3-dimensional collagen matrices,[22] highlighting a potential critical role of this gene in high-grade glioma. Because PI3K signaling plays a key role in numerous normal physiological processes and interference with this central pathway may thus lead to severe adverse effects, classifying PI3K downstream molecules, such as PDPN, as putative novel therapeutic targets for anti-cancer therapy is a matter of clinical concern.

In addition to genetic changes, hypermethylation of distinct CpG islands in the promoters of tumor-relevant genes, such as PDPN, plays an important role. We have identified a CpG island located in the proximal *PDPN* promoter that is critically involved in downregulation of PDPN expression by hypermethylation. This is confirmed by correlative evidence using DNA and RNA from primary human tumor samples and by functional analysis of the methylation pattern and the expression of PDPN in human glioma cell lines in the presence and absence of demethylating agents. Thus, we propose a model of PDPN regulation in human glioma involving both genetic and epigenetic mechanisms, as depicted in Fig. 7. Recently, Noushmehr et al. profiled promoter DNA methylation alterations in a large set of human glioblastoma samples in the context of The Cancer Genome Atlas. They identified a glioma-CpG island methylator phenotype (G-CIMP) in a subset of tumors with early onset, with significantly improved outcome, and with the characteristic presence of an IDH1 mutation. Of note, in this screen, PDPN was among the top-ranked hypermethylated genes with downregulated expression in G-CIMP tumors.[9] Epigenetic abnormalities play a major role in the development and progression of virtually all cancer types (for reviews see [47,56]). Currently, the attractive aim of epigenetic therapies is the reversibility of epigenetic changes that promote carcinogenesis: most importantly, the abnormal hypermethylation of tumor-suppressor genes resulting in their inactivation (for reviews see [56,57]). However, it should be taken into account that application of demethylating agents to patients with GB (i.e., with the G-CIMP signature) could increase the expression of genes involved in tumor progression and higher malignancy, such as PDPN. Thus, including protocols to eliminate high levels of PDPN expression may further increase the therapeutic efficiency of demethylating agents.

Supplementary Material

Supplementary material is available at *Neuro-Oncology Journal* online (http://neuro-oncology.oxfordjournals.org/).

Acknowledgments

We thank Alexander Biehler, Nataly Henfling, and Ingeborg Vogt for excellent technical assistance; Natalia Becker and Christian Schuster for help with statistical analyses; and Aurélie Ernst and Stefanie Krenzer for helpful discussion. The PTEN construct was kindly provided by H. Zentgraf (German Cancer Research

Center, Heidelberg, Germany) and the 5xTRE-luci and mutant 5xTRE-luci by M. Schorpp-Kistner (German Cancer Research Center, Heidelberg, Germany). The anti-mouse Pdpn monoclonal antibody (8.1.1) developed by Andrew Farr (Department of Biostructure, University of Washington, Seattle, WA, USA) was obtained from the Developmental Studies Hybridoma Bank, developed under the auspices of the NICHD and maintained by The University of Iowa, Department of Biology, Iowa City, IA, USA.

Conflict of interest statement. None declared.

Funding

This work was supported by the German Federal Ministry of Education and Research (BMBF) within the National Genome Research Network NGFNplus (01GS0883) to P.L., B.R. T.P., J.H., and P.A.

References

1. Ohgaki H, Kleihues P. Genetic alterations and signaling pathways in the evolution of gliomas. *Cancer Sci*. 2009;100(12):2235–2241.
2. Parsons DW, Jones S, Zhang X, et al. An integrated genomic analysis of human glioblastoma multiforme. *Science*. 2008;321(5897): 1807–1812.
3. Argyriou AA, Kalofonos HP. Molecularly targeted therapies for malignant gliomas. *Mol Med*. 2009;15(3–4):115–122.
4. Colman H, Zhang L, Sulman EP, et al. A multigene predictor of outcome in glioblastoma. *Neuro Oncol*. 2010;12(1):49–57.
5. Toedt G, Barbus S, Wolter M, et al. Molecular signatures classify astrocytic gliomas by IDH1 mutation status. *Int J Cancer*. 2011;128(5): 1095–1103.
6. Phillips HS, Kharbanda S, Chen R, et al. Molecular subclasses of high-grade glioma predict prognosis, delineate a pattern of disease progression, and resemble stages in neurogenesis. *Cancer Cell*. 2006;9(3): 157–173.
7. Verhaak RG, Hoadley KA, Purdom E, et al. Integrated genomic analysis identifies clinically relevant subtypes of glioblastoma characterized by abnormalities in PDGFRA, IDH1, EGFR, and NF1. *Cancer Cell*. 2010;17(1):98–110.
8. Van Meir EG, Hadjipanayis CG, Norden AD, Shu HK, Wen PY, Olson JJ. Exciting new advances in neuro-oncology: the avenue to a cure for malignant glioma. *CA Cancer J Clin*. 2010;60(3):166–193.
9. Noushmehr H, Weisenberger DJ, Diefes K, et al. Identification of a CpG island methylator phenotype that defines a distinct subgroup of glioma. *Cancer Cell*. 2010;17(5):510–522.
10. Matsui K, Breiteneder-Geleff S, Kerjaschki D. Epitope-specific antibodies to the 43-kD glomerular membrane protein podoplanin cause proteinuria and rapid flattening of podocytes. *J Am Soc Nephrol*. 1998;9(11):2013–2026.
11. Rishi AK, Joyce-Brady M, Fisher J, et al. Cloning, characterization, and development expression of a rat lung alveolar type I cell gene in embryonic endodermal and neural derivatives. *Dev Biol*. 1995;167(1): 294–306.
12. Zimmer G, Klenk HD, Herrler G. Identification of a 40-kDa cell surface sialoglycoprotein with the characteristics of a major influenza C virus receptor in a Madin-Darby canine kidney cell line. *J Biol Chem*. 1995;270(30):17815–17822.
13. Gandarillas A, Scholl FG, Benito N, Gamallo C, Quintanilla M. Induction of PA2.26, a cell-surface antigen expressed by active fibroblasts, in mouse epidermal keratinocytes during carcinogenesis. *Mol Carcinog*. 1997;20(1):10–18.
14. Scholl FG, Gamallo C, Vilaro S, Quintanilla M. Identification of PA2.26 antigen as a novel cell-surface mucin-type glycoprotein that induces plasma membrane extensions and increased motility in keratinocytes. *J Cell Sci*. 1999;112(Pt 24):4601–4613.
15. Kato Y, Fujita N, Kunita A, et al. Molecular identification of Aggrus/T1α as a platelet aggregation-inducing factor expressed in colorectal tumors. *J Biol Chem*. 2003;278(51):51599–51605.
16. Breiteneder-Geleff S, Soleiman A, Kowalski H, et al. Angiosarcomas express mixed endothelial phenotypes of blood and lymphatic capillaries: podoplanin as a specific marker for lymphatic endothelium. *Am J Pathol*. 1999;154(2):385–394.
17. Baluk P, McDonald DM. Markers for microscopic imaging of lymphangiogenesis and angiogenesis. *Ann N Y Acad Sci*. 2008;1131:1–12.
18. Makinen T, Norrmen C, Petrova TV. Molecular mechanisms of lymphatic vascular development. *Cell Mol Life Sci*. 2007;64(15):1915–1929.
19. Schacht V, Ramirez MI, Hong YK, et al. T1α/podoplanin deficiency disrupts normal lymphatic vasculature formation and causes lymphedema. *EMBO J*. 2003;22(14):3546–3556.
20. Raica M, Cimpean AM, Ribatti D. The role of podoplanin in tumor progression and metastasis. *Anticancer Res*. 2008;28(5B):2997–3006.
21. Wicki A, Christofori G. The potential role of podoplanin in tumour invasion. *Br J Cancer*. 2007;96(1):1–5.
22. Ernst A, Hofmann S, Ahmadi R, et al. Genomic and expression profiling of glioblastoma stem cell-like spheroid cultures identifies novel tumor-relevant genes associated with survival. *Clin Cancer Res*. 2009;15(21):6541–6550.
23. Durchdewald M, Angel P, Hess J. The transcription factor Fos: a Janus-type regulator in health and disease. *Histol Histopathol*. 2009;24(11):1451–1461.
24. Durchdewald M, Guinea-Viniegra J, Haag D, et al. Podoplanin is a novel fos target gene in skin carcinogenesis. *Cancer Res*. 2008;68(17):6877–6883.
25. Hummerich L, Muller R, Hess J, et al. Identification of novel tumour-associated genes differentially expressed in the process of squamous cell cancer development. *Oncogene*. 2006;25(1):111–121.
26. Louis DN, Ohgaki H, Wiestler OD, et al. The 2007 WHO classification of tumours of the central nervous system. *Acta Neuropathol*. 2007;114(2):97–109.
27. Liu HK, Belz T, Bock D, et al. The nuclear receptor tailless is required for neurogenesis in the adult subventricular zone. *Genes Dev*. 2008;22(18):2473–2478.
28. Angel P, Allegretto EA, Okino ST, et al. Oncogene jun encodes a sequence-specific trans-activator similar to AP-1. *Nature*. 1988;332(6160):166–171.
29. Offringa R, Gebel S, van Dam H, et al. A novel function of the transforming domain of E1a: repression of AP-1 activity. *Cell*. 1990;62(3): 527–538.
30. Hagmeyer BM, König H, Herr I, et al. Adenovirus E1A negatively and positively modulates transcription of AP-1 dependent genes by dimer-specific regulation of the DNA binding and transactivation activities of Jun. *EMBO J*. 1993;12(9):3559–3572.

31. Smeal T, Angel P, Meek J, Karin M. Different requirements for formation of Jun: Jun and Jun: Fos complexes. *Genes Dev*. 1989;3(12B):2091–2100.
32. Stein B, Baldwin AS, Jr, Ballard DW, Greene WC, Angel P, Herrlich P. Cross-coupling of the NF-κB p65 and Fos/Jun transcription factors produces potentiated biological function. *EMBO J*. 1993;12(10):3879–3891.
33. Ryffel GU, Kugler W, Wagner U, Kaling M. Liver cell specific gene transcription in vitro: the promoter elements HP1 and TATA box are necessary and sufficient to generate a liver-specific promoter. *Nucleic Acids Res*. 1989;17(3):939–953.
34. Ichimura K, Schmidt EE, Goike HM, Collins VP. Human glioblastomas with no alterations of the CDKN2A (p16INK4A, MTS1) and CDK4 genes have frequent mutations of the retinoblastoma gene. *Oncogene*. 1996;13(5):1065–1072.
35. van den Boom J, Wolter M, Kuick R, et al. Characterization of gene expression profiles associated with glioma progression using oligonucleotide-based microarray analysis and real-time reverse transcription-polymerase chain reaction. *Am J Pathol*. 2003;163(3):1033–1043.
36. Gentleman RC, Carey VJ, Bates DM, et al. Bioconductor: open software development for computational biology and bioinformatics. *Genome Biol*. 2004;5(10):R80.
37. Peterziel H, Sackmann T, Strelau J, et al. F-spondin regulates neuronal survival through activation of disabled-1 in the chicken ciliary ganglion. *Mol Cell Neurosci*. 2011;46(2):483–497.
38. Klucky B, Mueller R, Vogt I, et al. Kallikrein 6 induces E-cadherin shedding and promotes cell proliferation, migration, and invasion. *Cancer Res*. 2007;67(17):8198–8206.
39. Rong Y, Durden DL, Van Meir EG, Brat DJ. 'Pseudopalisading' necrosis in glioblastoma: a familiar morphologic feature that links vascular pathology, hypoxia, and angiogenesis. *J Neuropathol Exp Neurol*. 2006;65(6):529–539.
40. Abounader R, Ranganathan S, Kim BY, Nichols C, Laterra J. Signaling pathways in the induction of c-met receptor expression by its ligand scatter factor/hepatocyte growth factor in human glioblastoma. *J Neurochem*. 2001;76(5):1497–1508.
41. Koul D, Shen R, Shishodia S, et al. PTEN down regulates AP-1 and targets c-fos in human glioma cells via PI3-kinase/Akt pathway. *Mol Cell Biochem*. 2007;300(1–2):77–87.
42. Endersby R, Baker SJ. PTEN signaling in brain: neuropathology and tumorigenesis. *Oncogene*. 2008;27(41):5416–5430.
43. Koul D. PTEN signaling pathways in glioblastoma. *Cancer Biol Ther*. 2008;7(9):1321–1325.
44. Ishii N, Maier D, Merlo A, et al. Frequent co-alterations of TP53, p16/CDKN2A, p14ARF, PTEN tumor suppressor genes in human glioma cell lines. *Brain Pathol*. 1999;9(3):469–479.
45. Kolenda J, Jensen SS, Aaberg-Jessen C, et al. Effects of hypoxia on expression of a panel of stem cell and chemoresistance markers in glioblastoma-derived spheroids. *J Neurooncol*. 2011;103(1):43–58.
46. Feinberg AP. Phenotypic plasticity and the epigenetics of human disease. *Nature*. 2007;447(7143):433–440.
47. Ting AH, McGarvey KM, Baylin SB. The cancer epigenome–components and functional correlates. *Genes Dev*. 2006;20(23):3215–3231.
48. Brennan C, Momota H, Hambardzumyan D, et al. Glioblastoma subclasses can be defined by activity among signal transduction pathways and associated genomic alterations. *PLoS One*. 2009;4(11):e7752.
49. Brennan C. Genomic profiles of glioma. *Curr Neurol Neurosci Rep*. 2011;11(3):291–297.
50. Bunney TD, Katan M. Phosphoinositide signalling in cancer: beyond PI3K and PTEN. *Nat Rev Cancer*. 2010;10(5):342–352.
51. Chen R, Nishimura MC, Bumbaca SM, et al. A hierarchy of self-renewing tumor-initiating cell types in glioblastoma. *Cancer Cell*. 2010;17(4):362–375.
52. Atsumi N, Ishii G, Kojima M, Sanada M, Fujii S, Ochiai A. Podoplanin, a novel marker of tumor-initiating cells in human squamous cell carcinoma A431. *Biochem Biophys Res Commun*. 2008;373(1):36–41.
53. Courtney KD, Corcoran RB, Engelman JA. The PI3K pathway as drug target in human cancer. *J Clin Oncol*. 2010;28(6):1075–1083.
54. Ihle NT, Powis G. Inhibitors of phosphatidylinositol-3-kinase in cancer therapy. *Mol Aspects Med*. 2010;31(2):135–144.
55. Waldner MJ, Neurath MF. The molecular therapy of colorectal cancer. *Mol Aspects Med*. 2010;31(2):171–178.
56. Lechner M, Boshoff C, Beck S. Cancer epigenome. *Adv Genet*. 2010;70:247–276.
57. Mani S, Herceg Z. DNA demethylating agents and epigenetic therapy of cancer. *Adv Genet*. 2010;70:327–340.